Physics Letters A ••• (••••) •••–•••

Contents lists available at ScienceDirect

Physics Letters A

www.elsevier.com/locate/pla

Perfect spin filtering effect in ultrasmall helical zigzag graphene nanoribbons

Zi-Yue Zhang

Department of Applied Physics, Jiangnan University, Wuxi, Jiangsu Province 214121, China

ARTICLE INFO

Article history:
Received 13 October 2016
Received in revised form 7 November 2016
Accepted 29 November 2016
Available online xxxx
Communicated by R. Wu

Keywords:
???

ABSTRACT

The spin-polarized transport properties of helical zigzag graphene nanoribbons (ZGNRs) are investigated by first-principles calculations. It is found that although all helical ZGNRs have similar density of states and edge states, they show obviously different transport characteristics depending on the curling manners. ZGNRs curled along zigzag orientation exhibit perfect spin filtering effect with a large spin-split gap near the Fermi level, while ZGNRs curled along armchair orientation behave as conventional conductors for both two spin channels. The spin filtering effect will be weakened with the increase of either ribbon width or curling diameter. The results suggest that ultrasmall helical ZGNRs have important potential applications in spintronics and flexible electronics.

1. Introduction

As an atomically thin two-dimensional (2D) material, graphene has ignited tremendous research interests owing to its exceptional electronic, optoelectronic, mechanical and transport properties [1–6]. However, the application of 2D graphene is unfortunately limited by their nature of zero-gap. One of successful attempts to overcome this problem is patterning the 2D graphene into nanometer-wide graphene nanoribbons (GNRs) [7–10]. Due to edge effects, GNRs demonstrate many intriguing properties, such as energy gap dependence of widths and crystallographic orientations [7–9], ballistic transport [11,12], zero-conductance resonance [13], half-metallic conduction [14], and valley filtering [15].

Most of previous studies originate often from GNRs without distortions. But there actually exist large numbers of strains in either free-standing or supported GNRs, which affect electronic structures and transport properties [10,16]. Twisting that has been observed experimentally is a specific deformation unique to GNRs [10]. Recently, the theory and experimental studies both presented spontaneous twisting or curling of GNRs driven by edge stresses [17–20], indicating that narrow ribbons could in fact be helical depending on size and edge species. Particularly, helical GNRs can be fabricated encapsulated in carbon nanotubes [21–23] or in chemically etched GNRs [24]. The effect of twisting on the electronic properties of armchair [18,25,26] and zigzag GNRs [27,28] (AGNR and ZGNR) has also been investigated using density functional theory calculations, respectively.

In this work, we focused on helical GNRs than 180°-twisted structures which were studied in previous works. The morphological transformation from twisted ribbons into helical ribbons have been direct observed in experiment [29] and many types of helical nanoribbons have been fabricated so far [30,31]. Since zigzag edges will induce magnetism which originates from the spin polarized edge states [14], it will be necessary and interesting to examine the transport properties of helical ZGNRs. It turned out that particular and intriguing spin filtering effects are presented for helical ZGNRs twisted along zigzag orientation, a rarity in previous 180°-twisted ZGNRs and pristine ZGNRs [28,32–34]. The spin filtering effect promises helical ZGNRs great prospect for further development in novel flexible electronics and smart spintronic devices.

2. Computational methods and models

We refer to a H-terminated ZGNR with n zigzag carbon chains across the ribbon width as a Z_nGNR. Taking any imaginary infinite long nanotube as an axis, a Z_nGNR can twist along the tube wall forming helical nanoribbon like solenoid, as shown in Fig. 1(a). These helical nanoribbons can be classified by the tube diameter (d) and tube orientation (θ) that is denoted by the angle between tube and ribbon axis. Two series typical helical Z_nGNRs, Z-Z_nGNRs ($\theta = 30°$) and A-Z_nGNRs ($\theta = 60°$), are considered here. For convenient calculations, a carbon nanotube (CNT) is selected as the imaginary tube, thus the helical ribbons seems like cut-

E-mail address: zzy8423@jiangnan.edu.cn.

http://dx.doi.org/10.1016/j.physleta.2016.11.044
0375-9601/

ting from the tube wall. Their curling diameters are represented by the chiral of CNTs (m_1, m_2). For example, Fig. 1(b) and (d) shows Z-Z_6GNR curled around CNT (8, 0) [$Z_{(8,0)}$-Z_6GNR] and A-Z_6GNR curled around CNT (8, 8) [$A_{(8,8)}$-Z_6GNR], respectively. The ribbon twisting process is similar to rolling up the ribbon into a nanotube without two terminals of ribbon connecting with each other. In order to avoid the overlap of the ribbon, the curling diameter of A-Z_nGNR and Z-Z_nGNR should be larger than $1.356*n$ Å and $0.783*n$ Å in principle, respectively.

All the structures were relaxed using the conjugate gradient method in Vienna *ab initio* simulation package [35–37] until the force on each atom is less than 0.1 eV/nm. Based on the density functional theory (DFT) [38], the generalized gradient approximation (GGA) is employed for exchange-correlation potential. The energy cutoff is chosen to 300 eV and the Brillouin zone is sampled with $1 \times 1 \times 26$ Monkhorst meshes. The relaxations were realized by constraining the two ends of helical ribbons. As a consequence, semi-infinite CNTs with the same size to the imaginary tube were used for the electrodes. The quantum transport properties were calculated by TRANSIESTA [39] based on non-equilibrium Green's function techniques and the density-functional theory. The calculation details were in well accordance with the structural optimization. The current through the scattering region is calculated using the Landauer–Buttiker formula,

$$I(V_b) = G_0 \int_{\mu R}^{\mu L} T(E, V_{bias}) dE,$$

where $G_0 = 2(e^2/h)$ is the unit of quantum conductance and $T(E, V_{bias})$ is the transmission probability of electrons incident at energy E under potential bias V_{bias}. The electrochemical potential difference between two electrodes is $eV_{bias} = \mu L - \mu R$.

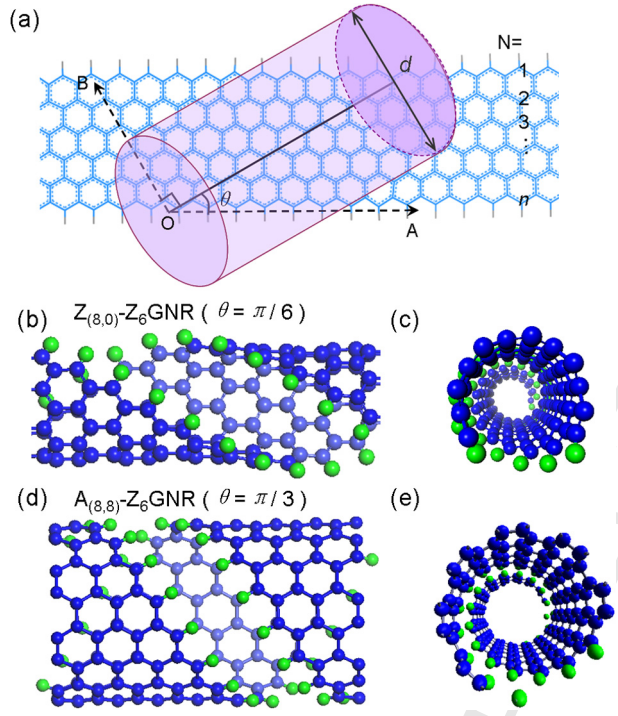

Fig. 1. (a) Schematic configuration of a H-terminated ZGNR twisting along the tube wall. OA and OB represents the length orientation of the ZGNR and diameter orientation of the tube, respectively. d and θ denotes the tube diameter and tube orientation, respectively. (b) Side view and (c) top view of $Z_{(8,0)}$-Z_6GNR. (d) Side view and (e) top view of $A_{(8,8)}$-Z_6GNR. Blue and green balls stand for carbon and hydrogen atoms, respectively. (For interpretation of the references to color in this figure legend, the reader is referred to the web version of this article.)

3. Results and discussions

The optimized atomic geometries of $A_{(8,8)}$-Z_6GNR and $Z_{(8,0)}$-Z_6GNR with fixed lengths of unit cells are shown in Fig. 1. It is interesting to find that two edges of $Z_{(8,0)}$-Z_6GNR buckle outwards obviously, while those of $A_{(8,8)}$-Z_6GNR do not. Some optimized structure parameters (Fig. S1) for $Z_{(8,0)}$-Z_6GNR and $A_{(8,8)}$-Z_6GNR can be compared with pristine Z_6GNR in Table SI. Relatively to $A_{(8,8)}$-Z_6GNR, the bond lengths and angles near the edges of $Z_{(8,0)}$-Z_6GNR are both more sensitive to the geometry optimization. The similar results can also be found in other sizes of helical ZGNRs. Due to the existence of edge buckling, it is necessary to examine the edge stability of helical Z_nGNR by calculating their edge energies per edge atom. The edge energy accounting for the energy cost to create an edge defines the edge chemical stability, which is calculated as $E_{\text{edge}} = (E_{\text{tot}} - N_C E_C - N_H E_H)/N_C^{\text{edge}}$, where N_C, N_H and N_C^{edge} are the number of carbon, hydrogen and carbon edge atoms per unit cell, respectively. E_{tot} is the total energy per unit cell of the helical Z_nGNR, while E_C and E_H are the cohesive energies of a carbon atom in graphene and a hydrogen atom in H_2 molecule, respectively. As shown in Fig. 2, the edges of helical Z_nGNRs at the antiferromagnetic (AFM) state are more stable than ferromagnetic (FM) state. Edge energies are reduced monotonously with increasing the ribbon width or curling diameter. Z-Z_nGNR exhibits much higher edge stability than A-Z_nGNR with the same ribbon width and similar curling diameter due to edges deformation discussed above. Clearly, twist strain brings the rise of edge instability, where edge energies of $Z_{(8,0)}$-Z_nGNRs and $A_{(8,8)}$-Z_nGNRs are about 0.1 eV and 0.5 eV higher than the pris-

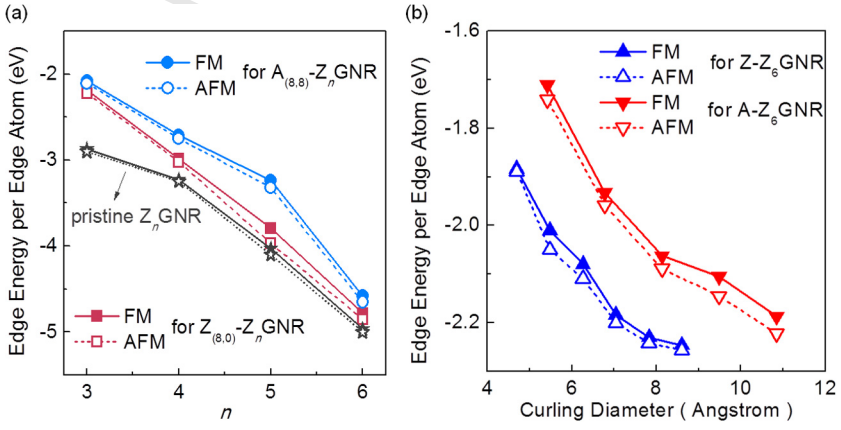

Fig. 2. Edge energies as functions of (a) ribbon widths (represents by parameter n) and (b) curling diameter.